AIP | Applied Physics Letters

Phase transitions and thermotropic phase boundaries in MnO2-doped (K0.5Na0.5)NbO3-0.05LiNbO3 single crystals: Raman scattering evidence at elevated temperatures

L. P. Xu, K. Jiang, J. Z. Zhang, G. S. Xu, Z. G. Hu, and J. H. Chu

Citation: Applied Physics Letters **106**, 122901 (2015); doi: 10.1063/1.4916226
View online: http://dx.doi.org/10.1063/1.4916226
View Table of Contents: http://scitation.aip.org/content/aip/journal/apl/106/12?ver=pdfcov
Published by the AIP Publishing

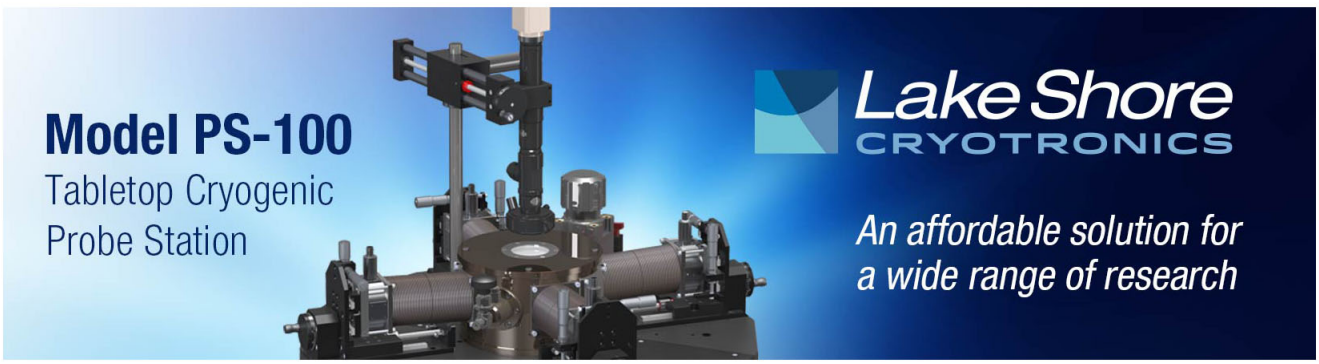

Phase transitions and thermotropic phase boundaries in MnO_2-doped $(K_{0.5}Na_{0.5})NbO_3$-0.05$LiNbO_3$ single crystals: Raman scattering evidence at elevated temperatures

L. P. Xu (徐丽萍),[1] K. Jiang (姜凯),[1,2] J. Z. Zhang (张金中),[1,2] G. S. Xu (许桂生),[3] Z. G. Hu (胡志高),[1,a)] and J. H. Chu (褚君浩)[1]
[1]*Key Laboratory of Polar Materials and Devices, Ministry of Education, Department of Electronic Engineering, East China Normal University, Shanghai 200241, China*
[2]*National Laboratory for Infrared Physics, Shanghai Institute of Technical Physics, Chinese Academy of Science, Shanghai 200083, China*
[3]*Key Laboratory of Transparent Opto-Functional Advanced Inorganic Materials, Shanghai Institute of Ceramics, Chinese Academy of Sciences, Shanghai 201899, China*

(Received 7 February 2015; accepted 14 March 2015; published online 23 March 2015)

Raman scattering of $(K_{0.5}Na_{0.5})NbO_3$-0.05$LiNbO_3$-yMnO_2 (y = 0% and 1.0%) single crystals have been reported in the temperature range from 300 to 800 K. The spectra exhibit a competition between a soft mode and a relaxation mode upon heating across the diverse transitions. The progressive change in the conflicting displacive mechanism (soft mode) and order-disorder (relaxation mode) can explain the origin of the successive orthorhombic-tetragonal-cubic phase transitions. Moreover, the polymorphic phase transition between orthorhombic and tetragonal structures can be confirmed through the observation of thermotropic phase boundaries for MnO_2-doped $(K_{0.5}Na_{0.5})NbO_3$-0.05$LiNbO_3$ single crystals. © *2015 AIP Publishing LLC*.
[http://dx.doi.org/10.1063/1.4916226]

Potassium sodium niobate [$(K_{0.5}Na_{0.5})NbO_3$: KNN] has been recognized as a potential alternative for $Pb(Zr_xTi_{1-x})O_3$ (PZT) because of its relatively strong piezoelectric properties and high Curie temperature (T_c) of 693 K.[1,2] Recently, KNN based lead-free materials were reported to offer comparable piezoelectric properties to that of PZT, such as KNN-$LiNbO_3$,[3] KNN-$LiTaO_3$,[4] KNN-$LiSbO_3$,[5] and KNN-$(Bi_{0.5}Na_{0.5})TiO_3$.[6] Among modified KNN based materials, single crystals might have better piezoelectricity than the textured ceramics counterpart, because the optimal crystallographic orientation and domain engineering can be realized in single crystals. Therefore, more fundamental researches on KNN-based single crystals are urgently needed to be carried out. $(K_{0.5}Na_{0.5})NbO_3$–0.05$LiNbO_3$ (KNN-LN) single crystals were grown by Bridgman method.[7] The single crystals show a high d_{33} on the order of 205–405 pC/N, with a T_c of 697 K. However, one of the problems to be overcome is a relatively high leakage current due to surface defects.[8,9] MnO_2 is one of the most interesting and useful additives, because Mn can exhibit three valences of 2+, 3+, and 4+. In the case of MnO_2 substitution for KNN-LN, Mn acts as electron or hole absorbant with the increase of Mn valence during oxidation, and oxygen occupies oxygen vacancies, followed by the formation of electron-hole.[10] The doping of Mn is shown to be effective for improving polarization and leakage current properties.

In the previous reports, all of the modifications in KNN were reported to exhibit enhanced piezoelectric properties due to the formation of morphotropic phase boundary (MPB).[3,4] However, it has been now thought that the highest piezoelectric properties are observed near a polymorphic phase transition (PPT) between tetragonal (T) and orthorhombic (O) phases at room temperature.[11] Note that the MPB region of PZT is nearly vertical in the temperature-composition phase diagram.[12] In other words, the MPB region is nearly temperature independent. However, the PPT in KNN based materials is not vertical and shows strong temperature dependence. Thus, it is imperative for lead free piezoelectrics to identify phase diagrams for promising materials. Generally, Raman spectroscopy is a powerful tool for the study of structural phase transition, which can measure molecular vibrations directly and is very sensitive to nonuniform distortions of the crystal lattice in short-range ordering. Especially, the phonon frequencies as a function of temperature could be a crucial tool to investigate phase transition.[13,14] Recent reports have investigated phase transition in KNN-LN and related materials through the use of Raman spectroscopy.[2,11] However, no Raman scattering study has been reported on the physical mechanism what drives the phase transitions and the PPT for MnO_2 doped KNN-LN single crystals.

In this letter, phase transitions of KNN-LN based single crystals have been investigated by temperature-dependent Raman spectroscopy from 300 to 800 K. The phase mechanism is discussed in terms of a displacive/order-disorder crossover. We provide direct experimental evidence of the PPT in KNN-LN based single crystals. In particular, the thermotropic phase boundaries of KNN-LN based single crystals have been observed, which present unique opportunities for the design of green high-performance materials.

$(K_{0.5}Na_{0.5})NbO_3$–0.05$LiNbO_3$-yMnO_2 (y = 0% and 1.0%) single crystals were grown by flux-Bridgman method. The raw materials were high-purity (99.99%) powders of Na_2CO_3, K_2CO_3, Li_2CO_3, Nb_2O_5, and MnO_2. The powders were calcined in air at 800 °C for 2 h before being pressed at cold

a)Author to whom correspondence should be addressed. Electronic mail: zghu@ee.ecnu.edu.cn. Tel.:+86-21-54345150. Fax: +86-21-54345119.

isostatic of 200 MPa. In the $(K_{0.5}Na_{0.5})NbO_3$–0.05$LiNbO_3$-y MnO_2 crystals grown by flux-Bridgman method, the platinum crucibles were maintained at 1200 °C for more than 10 h and then descended at a rate of 0.2–0.4 mm/h. The temperature gradient of 30–50 °C/cm was used near the solid-liquid interface in the growth furnace. After the end of the crystal growth, the temperature of the growth furnace was cooled down at a rate of 100–200 °C/h to room temperature. We obtained some (001)-cut crystal plates from crystal boules.[10] In order to remove the surface overlayer artifacts in analyzing the Raman data, all single crystals were single-side polished along (001) with a mechanical polishing progress.

Temperature dependent Raman spectra were collected with a Jobin-Yvon LabRAM HR 800 micro-Raman spectrometer and a THMSE 600 heating/cooling stage (Linkam Scientific Instruments) in the temperature range from 300 to 800 K with a resolution of 0.1 K. A laser with the wavelength of 633 nm was used as the excitation source and the spectral resolution is better than 1 cm^{-1}. The laser power focused on the sample is estimated to about 4 mW. Therefore, the effect of the heating induced by the laser beam can be ignored. The laser beam was focused through a 50× microscope with a working distance of 18 mm. An air-cooled charge coupled device (CCD) was used to collect the scattered signal dispersed on 1800 grooves/mm grating in the frequency range of 10–1000 cm^{-1}. All spectra were corrected by the Bose-Einstein temperature factor to facilitate comparison and eliminate the contribution from the Bose Einstein population factor. In order to study the variation trend of phonon modes, Raman spectra were fitted with independent damped harmonic oscillators.

The X-ray diffraction (XRD) results indicate that both KNN-0.05LN and KNN-0.05LN-1%MnO_2 crystals have pure orthorhombic perovskite structures without other phases at room temperature.[10] Both KNN and LN have octahedral NbO_6 basic units in their crystals. KNN belongs to an orthorhombic perovskite structure with space group *Amm*2, and LN possess a trigonal ilmenite structure with space group *R*3c at room temperature.[15] A theoretical analysis predicts that KNN with space group *Amm*2 (C_{2v}^{14}) has Raman-active optical modes of $4A_1 \oplus 4B_1 \oplus 3B_2 \oplus A_2$, while *R*3c ($C_{3v}^{6}$) for LN has $4A_1 \oplus 5A_2 \oplus 9E$ modes. All of these modes except for the A_2 mode are also infrared active. The observed modes can be separated into translational modes of an isolated cation and internal modes of coordination polyhedra.[16] In that case, the vibrations of the NbO_6 octahedra is formed from $1A_{1g}(v_1) + 1E_g(v_2) + 2F_{1u}(v_3, \quad v_4) + 1F_{2g}(v_5) + 1F_{2u}(v_6)$. In order to confirm the interpretation of Raman spectra in KNN based single crystals, polarized Raman spectra were also measured (not shown). The cross (VH), parallel (VV), and non-polarized Raman spectra do not differ qualitatively expect for the intensity variations. It is probably ascribed to the existence of micropolar domains, which partly influences the vibrational properties, as well as the Raman selection rules. The obtained peak positions in orthorhombic KNN-LN crystals and the corresponding symmetry assignments at room temperature are listed in Table I.[15,17,18]

Figs. 1(a) and 1(b) depict temperature dependence of Raman scattering for the KNN-LN and KNN-LN-1%MnO_2 crystals, respectively. Some remarkable differences could be observed between Raman spectra of KNN-LN and KNN-LN-1%MnO_2 at room temperature. The peak centered at about 190 cm^{-1} becomes noticeable, and the splitting peaks are more clear in the frequency range between 250 and 300 cm^{-1} due to the doping of MnO_2. However, the separation into two peaks is more apparent around 600 cm^{-1} in KNN-LN. The phase structure of KNN-LN based crystals transforms from O phase to T phase, then to cubic (C) phase with increasing temperature. For the O, T, and C phases, the frequencies from almost all of the phonon modes shift to lower wavenumbers and the intensities of all major peaks reduce with increasing temperature. It is thermal unit-cell expansion, which leads to elongation of the chemical bonds, which results in lower frequency of the corresponding Raman peaks. The distinct spectral changes across the O-T phase transition boundary are apparent. The peaks around 250 and 600 cm^{-1} obviously shift to higher frequencies. A dynamic central peak (CP) is observed across the transition from low-temperature to T phase, as shown in Fig. 1. Additionally, the phase transition from the O to T phase is initiated at 410 K and completed above 420 K for KNN-LN. In other words, a PPT between O and T phases is found for KNN-LN in the temperature range from 410 to 420 K. However, the PPT is not obvious in KNN-LN-1%MnO_2. Note that the spectral changes across the T-C phase transition boundary are also evident. Just below the transition, the T phase has strong broad modes at 250 and 600 cm^{-1} and weaker modes at 25 and 850 cm^{-1}. The two strong modes broaden and weaken above T_c, and these weak modes disappear completely.

The disorder in the O, T, and C phases can be characterized mainly by the Nb central ion allowed positions, then the framework of the established eight-site model will be adopted.[18] In the cubic paraelectric phase, the Nb ion may occupy any corner of a cube defined by eight equivalent sites along the [111] axes. In the T and O phases, four sites of a face of this cube and two sites of an edge may be occupied, respectively. In order to obtain a complete description of the dynamical properties through the successive phase transitions, it is useful to know the classification of the optical

TABLE I. The phonon frequencies and the symmetry assignments in orthorhombic KNN-LN based single crystals (in cm^{-1}, at 300 K). Note that the error bars are presented in parentheses.

Raman mode	B_2 (TO)	B_1 (TO)	B_2 (TO)	A_1 (TO)	B_1 (TO)	B_1 (TO)	A_2 (TO)	A_1 (TO)	B_2 (TO)	B_1 (TO)	A_1 (TO)	$B_1 + B_2 + A_1$ (LO)
KNN–LN	64	115	142	199	234	250	263	276	565	612	628	863
	(0.3)	(1.8)	(1.4)	(1.7)	(1.1)	(1.4)	(0.8)	(0.6)	(0.2)	(0.8)	(0.2)	(0.9)
KNN–LN–1%MnO_2	56	132	191	246	257	269	278	291	549	571	594	842
	(0.3)	(1.8)	(0.1)	(2.0)	(0.3)	(0.4)	(0.4)	(0.4)	(0.7)	(0.4)	(0.6)	(1.0)

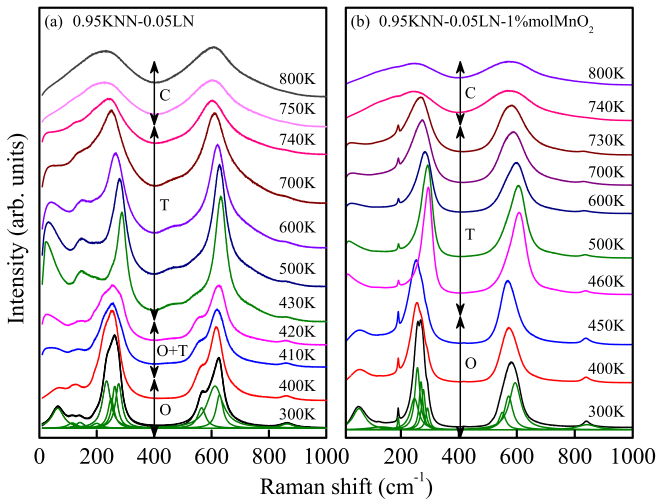

FIG. 1. Temperature dependence of Raman scattering for the KNN-LN based single crystals collected in the temperature range from 300 to 800 K and Lorentzian-shaped deconvolution at the temperature of 300 K. The arrows are applied to separate different phase transition.

modes and their correlations between the various phases.[19] In the cubic phase with space $Pm3m$ (O_h^1), the 12 optical phonons transform as the $3F_{1u}+F_{2u}$. The three F_{1u} phonons are labelled 1, 2, and 3 in order of increasing frequency and the F_{2u} phonon is labelled 4. The point groups of the ferroelectric phases are not subgroups of one another but all are subgroups of the cubic group. Consequently, the modes are grouped according to the cubic phonons, from which they are derived. The transformations of these modes in the various structures and phase transition temperatures on heating are recalled in Table II.

For a closer inspection, the peak positions of all modes in each phase are plotted in Fig. 2 against the temperature between 300 and 800 K. Frequency shifts and transformations of the modes are clear at the O-T and T-C boundaries. The trends within each phase consist primarily of mode softening with increasing temperature, exactly as expected to follow from the lattice thermal expansion. It is worth to note that B_2 ($\sim$60 cm^{-1}) and CP ($\sim$25 cm^{-1}) modes, and the mode near 120 cm^{-1} anomalously harden with temperature from the orthorhombic to the cubic phase across the successive transitions. Since the B_2 ($\sim$60 cm^{-1}) phonon is related to the successive ferroelectric phase changes, it is called as the ferroelectric soft mode. In addition, the anomalies of the modes around 300 cm^{-1} in KNN-LN and between 240 and 300 cm^{-1} in the doped sample in the temperature range of 600–700 K may be due to the changes of domain microstructure. In the O phase, the dynamic behavior is dominated by the soft phonon since no CP is detected. Regarding the O-T phase transition, a CP is considered instead of the soft phonon mode. The CP is probably associated with a relaxation mode due to an intrinsic disorder in the lattice.[20] This disorder can be provided by the motion of the Nb ion between several possible off-center positions. It should be noted that the mixed-phase region (i.e., PPT) between orthorhombic and tetragonal phases is apparent in KNN-LN. In the mixed-phase region, the coexistence of a relaxation mode and a soft phonon is observed. In the T-C transition, the CP disappears and the soft phonon [$F_{1u}(TO_1)$] is regained. Three broad Raman modes located at around 120, 240, and 600 cm^{-1} in the cubic phase are a clear signal for disorder of the central ion. According to symmetry selection rules, no first-order Raman scattering should be observed. Because of the disorder of the central ion, which breaks the crystal inversion symmetry, dynamical distortions of the cubic structure are created. In the light of all the results, displacive and order-disorder mechanisms have to be associated in the description of the phase transitions. Thus, the successive phase transitions in KNN-LN based single crystals derive from competition between a soft phonon mode and a relaxation mode.

TABLE II. Correlation of the phonon symmetry for the various structures and transition temperatures through the phase sequence in KNN-LN based single crystals.

Orthorhombic	Tetragonal	Cubic
$Bmm2$ (C_{2v}^{14})	$P4mm$ (C_{4v}^1)	$Pm3m$ (O_h^1)
$3A_1+3B_1+3B_2$	$3A_1+3E$	$3F_{1u}$
$A_1+B_1+A_2$	$E+B_1$	F_{2u}
Heating	T_{O-T} (K)	T_C (K)
KNN–LN	430	750
KNN–LN–1%MnO_2	460	740

The piezoelectric properties near the thermotropic phase boundaries are of specific interest. Thus, it is necessary to investigate the character of thermal phase boundaries. A mixture of the O and T phases is obvious at the O-T phase boundary in KNN-LN single crystal. To systematically investigate the sequence of phase transitions, the fractions of each phase are plotted in Fig. 3 against the temperature from 300 to 800 K. In order to obtain the phase fraction, we assume that one phase at thermal phase boundaries is a linear superposition of the spectra below and above phase boundaries. As shown in Figs. 3(c) and 3(d), the fitting Raman spectra at 410 K and 440 K in KNN-LN and KNN-LN-1%MnO_2, respectively, are displayed in comparison with the observed spectra at the same temperature. The fitting spectra are obtained from the linear superposition of the Raman spectra below and above phase boundaries followed by $I_{fit}=(1-r)I_{below}+rI_{above}$, where I_{fit} represents the fitted Raman spectra, $0\le r\le 1$, I_{below}, and I_{above} are Raman spectrum below and above phase boundaries, respectively. The coincidence of the experimental and the fitted Raman spectra is well for both samples, which strongly confirms the coexistence of the O and T phases at the thermal phase boundary from O to T phase.

As shown in Fig. 3(a), the O phase disappears gradually and the T phase begins to emerge (9%–29%) from 375 to 420 K. The process of phase transition from O to T phase completes at 430 K. As temperature is further increased, the T phase disappears and the C phase becomes a dominant phase (72%) at 750 K. As for KNN-LN-1%MnO_2, the mixed structure state is obtained over a wide temperature range from 325 to 450 K, T phase is always a minority phase (less than 10%). This agrees with the fact that, in the temperature range where the T phase is observed, macroscopic properties of the phonon modes are consistent with an O phase. In the T-C phase boundary, the T phase disappears and turns into the C phase at 740 K. It can be said that KNN-LN-yMnO_2 crystals are transitional ferroelectrics between typical normal

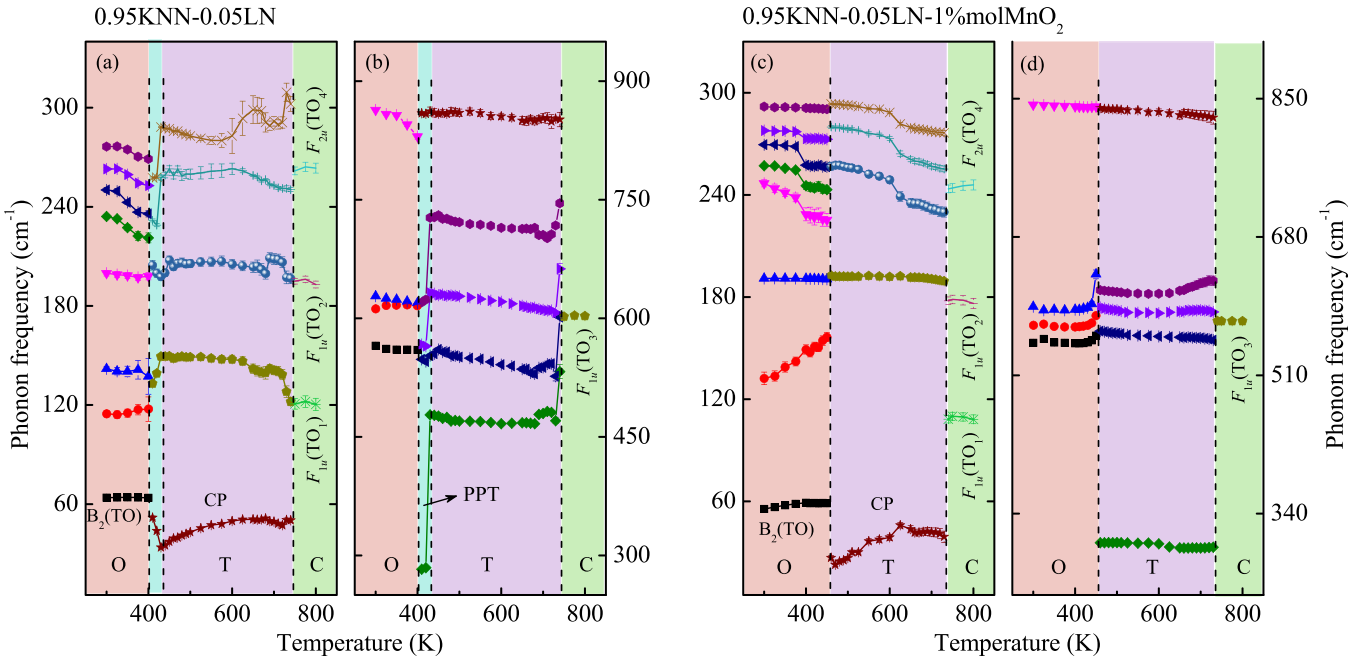

FIG. 2. Temperature dependence of the phonon frequency from KNN-LN based crystals. (a) and (c) The low frequency range of 10–300 cm^{-1}, (b) and (d) the high frequency range of 400–900 cm^{-1}. Note that different shade regions indicate that the crystals are located in diverse phase.

ones and typical relaxor ones, while the normal one is predominant. The mixed structure state at the thermal phase boundaries is due to sufficient competing mechanical and dipolar interactions between domains in multi-domain configurations.[21] In single domain case, the system undergoes a series of first-order ferroelectric transitions upon heating, sequentially adopting the O and T ferroelectric phases before reverting to the C parent phase.

In summary, temperature dependence of the mode frequencies through the successive phase transitions has been reported. The behavior of the phonon frequencies for soft mode and central peak shows the coexistence of displacive and disorder features in the diverse phase transitions. The competition between a soft mode and a relaxation mode is suggested to explain the mechanism of the phase transitions. Moreover, the thermotropic phase boundaries are observed, indicating the existence of the mixed-phase region (i.e., PPT) between orthorhombic and tetragonal phases.

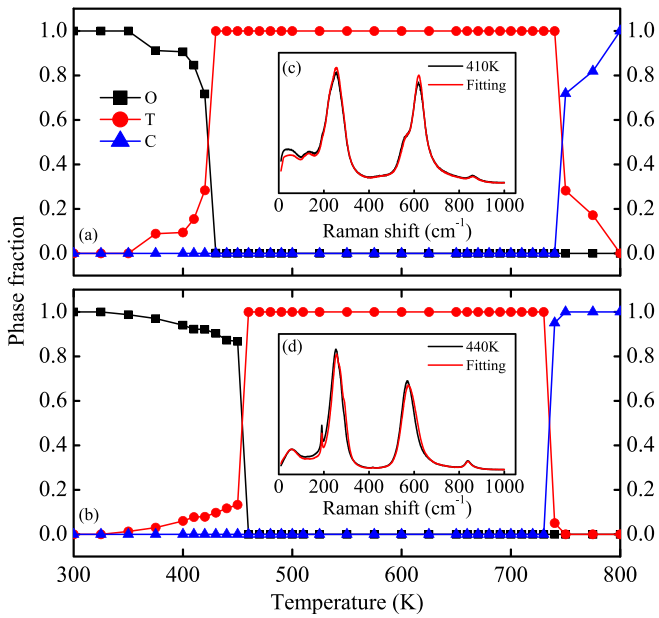

FIG. 3. Phase fraction of (a) KNN-LN and (b) KNN-LN-1%MnO_2 single crystals as a function of temperature. Note that (c) and (d) is the fitting Raman spectra at 410 K and 440 K for KNN-LN and KNN-LN-1%MnO_2, respectively.

This work was financially supported by Major State Basic Research Development Program of China (Grant Nos. 2011CB922200 and 2013CB922300), Natural Science Foundation of China (Grant Nos. 11374097 and 61376129), Projects of Science and Technology Commission of Shanghai Municipality (Grant Nos. 14XD1401500, 13JC1402100, and 13JC1404200), and the Program for Professor of Special Appointment (Eastern Scholar) at Shanghai Institutions of Higher Learning.

[1]Y. Saito, H. Takao, T. Tani, T. Nonoyama, K. Takatori, T. Homma, T. Nagaya, and M. Nakamura, Nature (London) **432**, 84 (2004).
[2]H. J. Trodahl, N. Klein, D. Damjanovic, N. Setter, B. Ludbrook, D. Rytz, and M. Kuball, Appl. Phys. Lett. **93**, 262901 (2008).
[3]Y. P. Guo, K. Kakimoto, and H. Ohsato, Appl. Phys. Lett. **85**, 4121 (2004).
[4]Y. J. Dai, X. W. Zhang, and G. Y. Zhou, Appl. Phys. Lett. **90**, 262903 (2007).
[5]S. J. Zhang, R. Xia, T. R. Shrout, G. Z. Zang, and J. F. Wang, J. Appl. Phys. **100**, 104108 (2006).
[6]R. Z. Zuo, X. S. Fang, and C. Ye, Appl. Phys. Lett. **90**, 092904 (2007).
[7]K. Chen, G. S. Xu, D. F. Yang, X. F. Wang, and J. B. Li, J. Appl. Phys. **101**, 044103 (2007).
[8]G. Shirane, R. Newnham, and R. Pepinsky, Phys. Rev. **93**, 672 (1954).
[9]Y. Kizaki, Y. Noguchi, and M. Miyayama, Appl. Phys. Lett. **89**, 142910 (2006).
[10]Y. Liu, G. S. Xu, J. F. Liu, D. F. Yang, and X. X. Chen, J. Alloys Compd. **603**, 95 (2014).
[11]N. Klein, E. Hollenstein, D. Damjanovic, H. J. Trodahl, N. Setter, and M. Kuball, J. Appl. Phys. **102**, 014112 (2007).

[12]T. R. Shrout and S. J. Zhang, J. Electroceram **19**, 113 (2007).
[13]Y. Y. Liao, Y. W. Li, Z. G. Hu, and J. H. Chu, Appl. Phys. Lett. **100**, 071905 (2012).
[14]L. P. Xu, L. L. Zhang, X. L. Zhang, J. Z. Zhang, Z. G. Hu, J. Yu, and J. H. Chu, J. Appl. Phys. **116**, 164103 (2014).
[15]K. Kakimoto, K. Akao, Y. P. Guo, and H. Ohsato, Jpn. J. Appl. Phys., Part 1 **44**, 7064 (2005).
[16]L. J. Hu, Y. H. Chang, M. L. Hu, M. W. Chang, and W. S. Tse, J. Raman Spectrosc. **22**, 333 (1991).
[17]A. V. Postnikov and G. Borstel, Phys. Rev. B **50**, 758 (1994).
[18]Ph. Pruzan, D. Gourdain, and J. C. Chervin, Phase Transitions **80**, 1103 (2007).
[19]M. D. Fontana, G. Métrat, J. L. Servoin, and F. Gervais, J. Phys. C **17**, 483 (1984).
[20]M. D. Fontana, A. Ridah, G. E. Kugel, and C. Carabatos-Nedelec, J. Phys. C **21**, 5853 (1988).
[21]T. T. A. Lummen, Y. J. Gu, J. J. Wang, S. M. Lei, F. Xue, A. Kumar, A. T. Barnes, E. Barnes, S. Denev, A. Belianinov, M. Holt, A. N. Morozovska, S. V. Kalinin, L. Q. Chen, and V. Gopalan, Nat. Commun. **5**, 3172 (2014).